Available online at www.sciencedirect.com
SCIENCE DIRECT
Nuclear Instruments and Methods in Physics Research B 242 (2006) 270–274
NIM B
Beam Interactions with Materials & Atoms
www.elsevier.com/locate/nimb

Improvement on corrosion resistance of NiTi orthopedic materials by carbon plasma immersion ion implantation

Ray W.Y. Poon [a], Joan P.Y. Ho [a], Camille M.Y. Luk [a], Xuanyong Liu [a], Jonathan C.Y. Chung [a], Paul K. Chu [a,*], Kelvin W.K. Yeung [b], William W. Lu [b], Kenneth M.C. Cheung [b]

[a] *Department of Physics and Materials Science, City University of Hong Kong, Tat Chee Avenue, Kowloon, Hong Kong*
[b] *Department of Orthopaedics and Traumatology, University of Hong Kong, Pokfulam, Hong Kong*

Available online 29 September 2005

Abstract

Nickel–titanium shape memory alloys (NiTi) have potential applications as orthopedic implants because of their unique super-elastic properties and shape memory effects. However, the problem of out-diffusion of harmful Ni ions from the alloys during prolonged use inside a human body must be overcome before they can be widely used in orthopedic implants. In this work, we enhance the corrosion resistance of NiTi using carbon plasma immersion ion implantation and deposition (PIII&D). Our corrosion and simulated body fluid tests indicate that either an ion-mixed amorphous carbon coating fabricated by PIII&D or direct carbon PIII can drastically improve the corrosion resistance and block the out-diffusion of Ni from the materials. Results of atomic force microscopy (AFM) indicate that both C_2H_2-PIII&D and C_2H_2-PIII do not roughen the original flat surface to an extent that can lead to degradation in corrosion resistance.

PACS: 52.77.Dq; 62.20.Dc; 64.70.Kb; 65.40.De

Keywords: NiTi shape memory alloys; Corrosion resistance; Surface morphology; Plasma immersion ion implantation and deposition

1. Introduction

The unique super-elastic properties and shape memory effects make nickel–titanium shape memory alloys (NiTi SMA) a good candidate for orthopedic implants. However, out-diffusion of harmful Ni from the NiTi substrate during prolonged use inside a human body is a serious issue [1] and the problem must be solved before the materials can be more widely used in orthopedics. In this work, we investigate the possibility of enhancing the surface anti-corrosion capability of NiTi shape memory alloys using carbon plasma immersion ion implantation and deposition (PIII&D) [2,3]. We used deposition produce hydrogenated amorphous carbon film on the NiTi surface and implantation to form an ion-mixed titanium carbide layer, respectively. In our first experiments, a graded C/NiTi interface was first produced followed by the deposition of an amorphous hydrogenated carbon film using radio-frequency (RF) C_2H_2 PIII&D. In our second set of experiments, carbon was implanted into the specimens using high-voltage glow discharge PIII in a C_2H_2 ambient. The surface structure, corrosion resistance and surface morphology of the materials treated by both methods are assessed and compared.

2. Experimental

Circular NiTi bars with 50.8% Ni (SE508 bar) were cut into discs 5 mm in diameter and 1 mm thick. They were grinded, polished to a shiny surface and then ultrasonically

* Corresponding author. Tel.: +852 2788 7724; fax: +852 2788 9549/7830.
E-mail address: paul.chu@cityu.edu.hk (P.K. Chu).

0168-583X/$ - see front matter © 2005 Elsevier B.V. All rights reserved.
doi:10.1016/j.nimb.2005.08.045

cleaned with acetone and ethanol before deposition or implantation was conducted in our plasma immersion ion implanter [4] with a vacuum chamber volume of 0.94 m^3. The deposition and implantation parameters are displayed in Table 1. In the deposition dominant experiments, a glow discharge [5] was first ignited in the C_2H_2 ambient at −30 kV for 20 min to produce a graded carbide layer to enhance film adhesion. Afterwards, the C_2H_2 plasma was sustained throughout the entire PIII&D process and so the primary process here (Sample #2 in Table 1) was deposition because the implantation duty cycle was very low. On the other hand, during the PIII only experiments (Sample #3 in Table 1), the C_2H_2 plasma was ignited by high-voltage glow discharge only when a high-voltage pulse was applied to the sample. The predominant process was thus ion implantation with very little deposition because there was no plasma formation between the high-voltage pulses.

The elemental depth profiles and Ti and C chemical states were determined by X-ray photoelectron spectroscopy (XPS) (Physical Electronics PHI 5802). The carbon chemistry was evaluated by Raman spectroscopy (Renishaw Raman System 2000) using a 514 nm Ar laser. The surface morphology of the treated and untreated control samples was examined by atomic force microscopy (AFM) (Autoprobe CP). Electrochemical tests based on ASTM G5-94 (1999) and G61-86 (1998) were performed by a potentiostat (VersaStat II EG&G) using a standard simulated body fluid (SBF) at a pH of 7.42 [6] and temperature of 37 ± 0.5 °C. A cyclic potential spanning between −400 mV and +1600 mV was applied at a scanning rate of 600 mV/h. Before the electrochemical tests, the medium was purged with nitrogen for 1 h to remove dissolved oxygen and nitrogen purging continued throughout the measurements. The SBF taken from each sample after the corrosion test was analyzed for Ni and Ti employing inductively coupled plasma mass spectrometry (ICPMS) (Perkin Elmer, PE SCIEX ELAN6100). To assess the surface morphology of the different samples, the electrochemical tests were performed again on another set of samples but this time the outer circular portion of the exposed sample surfaces were covered by nail polish. The surface morphology of each sample before and after the electrochemical test was evaluated under scanning electron microscopy (SEM) (SEM, JEOL JSM-820) after dissolving the nail polish in acetone.

Table 1
Deposition/implantation parameters

	Samples		
	#1	#2	#3
Description	Control	30 kV C_2H_2 Plasma deposition	40 kV C_2H_2 Plasma implantation
RF	–	500 W	–
High voltage	–	−30 kV	−40 kV
Pulse width	–	100 μs	30 μs
Frequency	–	100 Hz	200 Hz
Duration	–	90 min	90 min
Base pressure	–	1×10^{-5} Torr	1×10^{-5} Torr
C_2H_2 working pressure	–	3.8×10^{-4} Torr	2.0×10^{-3} Torr
Implant fluence	–	4.5×10^{16} cm^{-2}	5.5×10^{16} cm^{-2}
Vacuum annealing	–	–	1.0×10^{-5} Torr, 600 °C for 5 h

3. Results

Fig. 1 shows the XPS depth profiles obtained from the untreated control, deposited, as-implanted and implanted and annealed samples. The profiles have been plotted on a depth scale based on sputtering rates calculated from a SiO_2 reference under similar conditions for reference only, since it is well known that the sputtering rate changes in the surface region and is different from that of SiO_2. It is

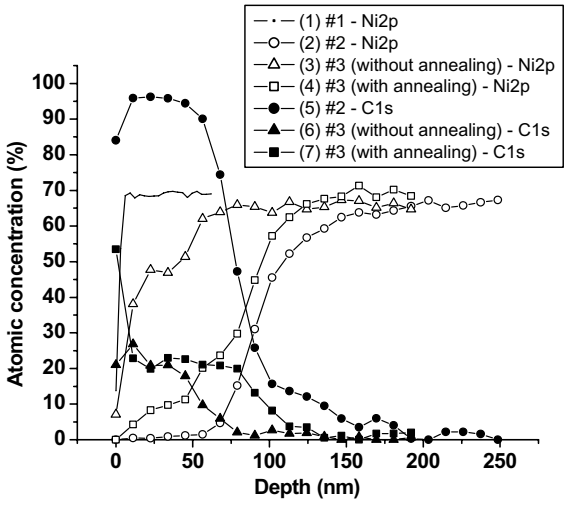

Fig. 1. XPS C and Ni depth profiles acquired from the NiTi, #1 (untreated), #2 (deposited without annealing) and #3 (implanted without annealing or with annealing).

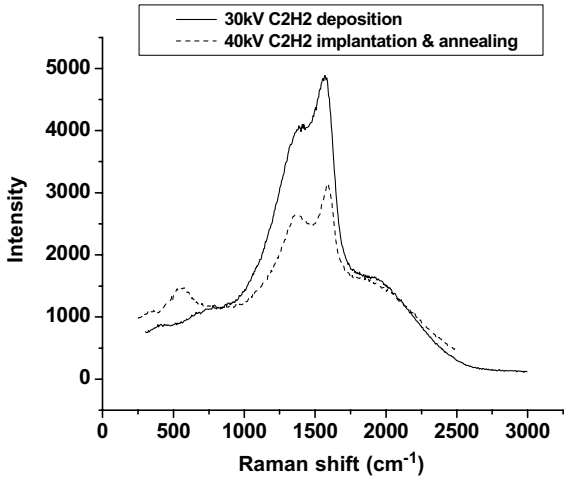

Fig. 2. Raman spectra of the treated NiTi alloys.

evident from the depth profiles that the Ni content is suppressed in the implanted region.

The Raman spectra from the deposited and implanted and annealed samples are displayed in Fig. 2. The spectra are representative of amorphous hydrogenated carbon and crystalline graphite, respectively and the latter exhibits well-resolved bands. The D-peak and G-peak positions of the deposited sample are 1397 cm^{-1} and 1582 cm^{-1}, respectively, whereas those of the implanted and annealed sample are 1378 cm^{-1} and 1593 cm^{-1}, respectively. The two bands become more separate and the results are consistent with those reported by Zhang and Koka [7]. Annealing thus not only promotes diffusion but also enhances crystallization.

The surface topographies of the untreated control, deposited and implanted and annealed samples are shown in Fig. 3(a)–(c) and Table 2 compares the root mean square (RMS) values of the surface roughness of the tested samples. The results show that the untreated control and the implanted and annealed samples have similar surface roughness, while the deposited sample is about twice as rough. However, it should be noted that the difference in the absolute roughness is quite small from the perspective of biomedical metals.

Table 2
Root mean square (RMS) values of surface roughness of the control and treated samples

Samples	RMS roughness (nm)
Control	4.3
30 kV C_2H_2 deposition	12.0
40 kV C_2H_2 implantation	5.3

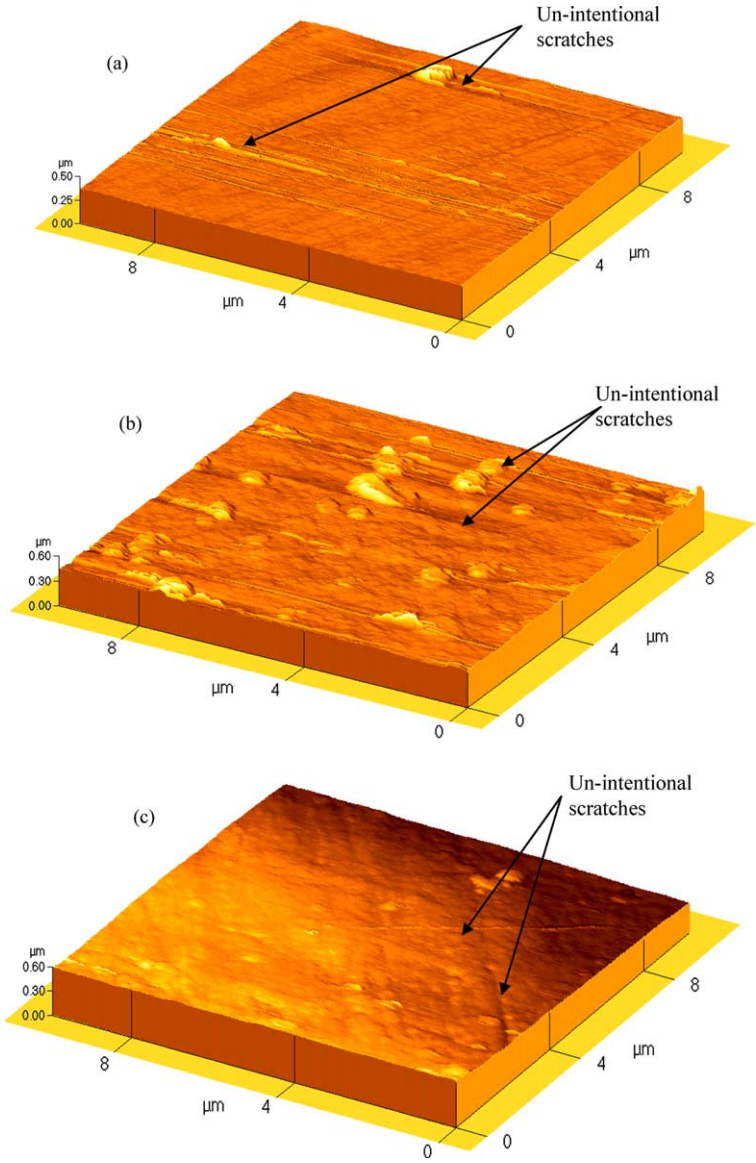

Fig. 3. AFM profiles acquired from the NiTi sample surfaces: (a) #1 (untreated), (b) #2 (deposited without annealing) and (c) #3 (implanted and annealed).

Table 3 summarizes the results of Ni and Ti concentrations in the SBF solutions determined by ICPMS after the electrochemical tests. Our data show that the amount of Ni leached from the control (untreated) sample during the electrochemical test is orders of magnitude higher than those detected from the deposited and implanted samples. The ICPMS results provide strong evidence that either PIII&D or PIII only can effectively block the out-diffusion of Ni from the NiTi shape memory alloys to the SBF.

Table 3
Amounts of Ni and Ti ions detected in SBF by ICPMS after electrochemical tests

Sample	Ni content (mg/l)	Ti content (mg/l)
#1	30.2324	0.1575
#2	⩽0.0056[a]	0.0228
#3	⩽0.0082[a]	0.057

Note: mg/l = ppm.
[a] Detection limited.

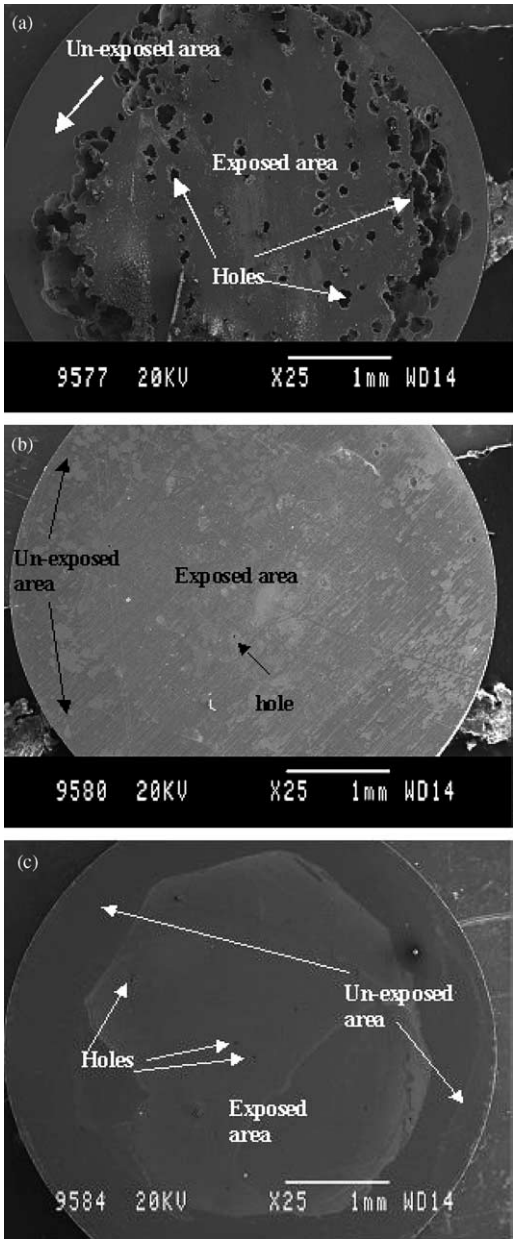

Fig. 4. SEM images after electrochemical tests (×25): (a) #1; (b) #2; (c) #3.

The morphology of the sample surfaces partially hidden by nail polish after the electrochemical tests is shown in Fig. 4. The SEM figures acquired after dissolving the nail polish by acetone show that there are very few tiny holes on the treated sample surfaces. In comparison, a large number of large and irregular holes can be observed on the surface of the untreated control sample. It is thus not coincidental that the amount of Ni ions leaching out from the control sample is orders of magnitude higher than those from the deposited and implanted and annealed samples.

4. Discussion

Fig. 1 shows a graded C/NiTi interface between 75 and 150 nm in the implanted sample. The high-resolution XPS analyses of the Ti 2p and C 1s at different sputtered depths (not shown here) show that within this range of sputtered depths, chemical shifts representative of carbide emerge revealing the existence of a graded carbide interface between the carbon film and substrate. This graded interface may enhance the film adhesion and mitigate film delamination. For the implanted and annealed sample, the shift from α-carbon to carbide occurs at 11 nm indicating that an implanted zone has been formed. High-resolution Ti 2p and C 1s spectra disclose the formation of titanium carbide layer with graded carbon. The suppression of the Ni content in the implanted region after annealing is consistent with previous results and can be attributed to the high affinity of titanium towards carbon and oxygen under high-temperature annealing [8]. The enhancement in the corrosion resistance of the carbon film and the titanium carbide layer may be attributed to the inherent chemical inertness of carbon, and the very strong and inert carbide bonds formed between titanium and carbon in the implanted samples. Oxygen was co-implanted into the samples as a result of the non-UHV (ultrahigh vacuum) implantation conditions in our PIII instrument [4] and may be beneficial to the anti-corrosion properties.

Annealing of TiC at high temperature, for instance, 600 °C in our experiments, may promote graphitization in which carbon atoms diffuse out from the carbide and form graphite [7]. Such a transition can be observed in Fig. 1. For the implanted and annealed sample, the carbon content at zero depth is higher than that of the as-implanted sample. Although annealing promotes graphitization, when monitoring the chemical shifts of the C 1s signal at different depth, increase in the carbon content can only be observed in the top 11 nm.

From Fig. 3 and Table 2, it is observed that C_2H_2-PIII basically does not roughen the originally flat surface,

whereas for C_2H_2-PIII&D, the deposited surface is rougher than those on the two other samples. It is likely that the surface roughness may alter the corrosion resistance of the materials. However, from our electrochemical tests, ICPMS analyses as well as SEM, both the deposited and implanted and annealed samples possess similarly improved anti-corrosion and diffusion barrier capabilities. It therefore appears that the small roughness difference does not degrade the corrosion resistance.

5. Conclusion

We have plasma deposited amorphous hydrogenated carbon thin films and plasma implanted carbon into NiTi substrates. The carbon coating formed on the substrate has a graded carbide interface thereby strengthening film adhesion. Titanium carbide is formed in the implanted samples. Both sets of samples exhibit better corrosion resistance compared to the untreated control sample based on our corrosion test and ICMPS analysis of the SBF although the deposited sample surface is a little rougher than the untreated control and the implanted sample surfaces. Thus, we have demonstrated that PIII&D is effective in improving the corrosion resistance of orthopedic NiTi shape memory alloys.

Acknowledgements

The work was jointly supported by Hong Kong Research Grants Council (RGC) Central Allocation Group Research Grant #CityU 1/04C and RGC Competitive Earmarked Research Grant (CERG) #HKU 7283/00M.

References

[1] A. Kapanen, J. Ilvesaro, A. Danilov, J. Ryhänen, P. Lehenkari, J. Tuukkanen, Biomaterials 23 (2002) 645.
[2] P.K. Chu, S. Qin, C. Chan, N.W. Cheung, L.A. Larson, Mater. Sci. Eng.: Rep. 17 (1996) 207.
[3] P.K. Chu, J. Vac. Sci. Technol. B 22 (2004) 289.
[4] P.K. Chu, B.Y. Tang, L.P. Wang, X.F. Wang, S.Y. Wang, N. Huang, Rev. Sci. Instr. 72 (2001) 1660.
[5] X.B. Tian, P. Peng, P.K. Chu, Phys. Lett. A 303 (2002) 1.
[6] S.B. Cho, K. Nakanishi, T. Kokubo, N. Soga, J. Am. Ceram. Soc. 78 (1995) 1769.
[7] L.H. Zhang, R.V. Koka, Mater. Chem. Phys. 57 (1998) 23.
[8] X.B. Tian, R.K.Y. Fu, L.W. Wang, P.K. Chu, Mater. Sci. Eng. A 316 (2001) 200.